

Metallization-induced spontaneous silicide formation at room temperature: The Fe/Si case

J. M. Gallego, J. M. García, J. Alvarez, and R. Miranda

Departamento de Física de la Materia Condensada, Universidad Autónoma de Madrid, Cantoblanco, 28049-Madrid, Spain

(Received 9 March 1992; revised manuscript received 2 July 1992)

The composition of the interface resulting from the room-temperature deposition of iron on Si(100) under ultrahigh-vacuum conditions has been monitored by surface-sensitive techniques such as Auger electron spectroscopy, low-energy electron diffraction, and photoemission spectroscopy with synchrotron radiation. The results show unequivocally that the Fe/Si interface is not abrupt, but rather an amorphous intermixed region with composition close to Fe_3Si . The formation of this silicidelike layer is related to the metallization of the deposited Fe overlayer. Upon annealing a thick film of Fe, we demonstrate that Fe_3Si is the first phase to nucleate, in opposition to standard models that point to FeSi as the first silicide formed.

INTRODUCTION

Recently a great deal of work has been dedicated to the growth and characterization of iron silicides. Most of this attention has centered in $\beta\text{-FeSi}_2$, the only iron silicide, and one of the few among the transition-metal silicides, known to be semiconducting, with a band gap, presumably direct, of ≈ 0.9 eV.^{1,2} In an attempt to improve the surface morphology and crystalline quality of $\beta\text{-FeSi}_2$ grown epitaxially on Si, the interest has shifted to characterize the Fe/Si interface and the first silicide formed during annealing under ultrahigh-vacuum (UHV) conditions. In spite of the work done,²⁻¹² contradictions abound. In particular, the sequence of phase formation is still unclear. In addition to basic issues, there are two practical reasons for which this information must be obtained. First, only with this information can the quantity of silicon consumed in the reaction be determined. The second is to allow prediction of the electrical characteristics of the silicide/silicon contacts.¹³

Early studies³ of the Fe/Si system using Rutherford backscattering spectrometry (RBS) and x-ray diffraction (XRD) showed that Fe_3Si and FeSi formed after annealing a 1340-Å Fe film on Si(100) at $\sim 450\text{--}525^\circ\text{C}$. At 550°C , an FeSi_2 phase grew between the Si substrate and the FeSi phase. The formation sequence was the same on Si(111), although the silicides formation rates were slightly faster. Transmission electron microscope investigations⁴ found that, for 300-Å Fe films deposited on Si and annealed in N_2 ambient, FeSi was formed at 400°C . Small amounts of Fe_3Si were observed at $450\text{--}500^\circ\text{C}$. Above 600°C , $\beta\text{-FeSi}_2$ was the dominant phase, while $\alpha\text{-FeSi}_2$ was observed only at 800°C . More recent XRD data⁵ have found that, for 1500-Å Fe films deposited on Si(100), Fe_3Si and FeSi appear after annealings at 600 and 700°C , respectively. At 750°C a mixture of FeSi and $\beta\text{-FeSi}_2$ is obtained, while for temperatures between 800 and 900°C only $\beta\text{-FeSi}_2$ is observed. At higher temperatures ($950\text{--}1100^\circ\text{C}$) the metallic $\alpha\text{-FeSi}_2$ is formed.

All experiments mentioned above were performed using conventional vacuum techniques. In UHV, and for much thinner Fe films (20–30 Å) deposited on Si(111),

Auger electron spectroscopy (AES) and electron energy-loss spectroscopy (EELS) (Refs. 9 and 10) show that FeSi is formed at temperatures ranging from 350 to 500°C , while $\beta\text{-FeSi}_2$ appears between 500 and 650°C . On Si(100), FeSi appears at $300\text{--}425^\circ\text{C}$, and FeSi_2 between 500 and 625°C .¹¹

While there is agreement in the fact that the formation temperature of the different phases depends on the vacuum conditions, the sequence of formation remains in dispute. Surprisingly, none of the measurements performed in UHV has detected the formation of Fe_3Si , while for films deposited under conventional vacuum it is normally found at temperatures lower than that where FeSi appears.

As we shall see, the first phase to nucleate during annealings of Fe/Si couples is closely related to the actual composition of the as-deposited Fe/Si interface. However, before the work at hand, the exact nature of this interface was disputed. On Si(111)(7×7) the LEED pattern corresponding to an Fe(111) bcc surface was observed when the thickness of the film became large enough (≈ 20 ML), which suggests that Fe forms on this surface an epitaxial layer.¹² Nevertheless, Auger data indicate a deviation from ideal layer-by-layer growth after the deposition of the second Fe layer. In spite of this, Urano *et al.*¹² claimed that the Fe/Si interface was abrupt. On the contrary, based on photoemission data, a thin, intermixed layer of $\beta\text{-FeSi}_2$ (Refs. 6 and 7) or FeSi (Ref. 8) has been proposed to exist at the Fe/Si interface. At very high coverages, a pure Fe overlayer has always been found.

In this paper, we report the growth and characterization of Fe on Si(100). Our results show that the Fe/Si interface at room temperature is far from being atomically abrupt. Rather, a mixed amorphous region forms which composition is close to Fe_3Si , and not FeSi_2 or FeSi as previously reported. Upon annealing a Fe/Si couple in UHV, we demonstrate that Fe_3Si is the first phase to nucleate.

EXPERIMENT

The experiments have been carried out in an UHV vacuum chamber equipped with surface-sensitive analytical

techniques such as AES, EELS, and LEED. The base pressure was 2×10^{-10} torr. After introduction in the vacuum chamber, and when the pressure was in the 10^{-10} range, the sample was annealed resistively for a few seconds to 1200°C, cooled quickly to 900°C, and then let slowly cooled to room temperature. This procedure always resulted in a clear and sharp 2×1 two-domain LEED pattern, while no traces of contamination (C,O) could be detected with AES. The temperature of the sample was measured with a Cr-Al thermocouple, and checked in the high-temperature range with an optical pyrometer.

Iron was evaporated from an Fe wire wrapped around a tungsten wire through which current passed. The pressure during evaporation did not exceed 2×10^{-9} torr. After each run of measurements, the sample was cleaned by cycles of Ar^+ sputtering and annealing until a sharp LEED pattern similar to that of the original surface was recovered and no Fe signal could be detected with AES.

The Auger spectra were taken with a single pass cylindrical mirror analyzer (CMA) equipped with a coaxial electron gun which provided a typical sample current of $\approx 1 \mu\text{A}$. The resolution of the analyzer, measured as the half-width of the elastic peak, was 0.7%. The spectra were taken in derivative mode, modulating the voltage ramp ($1 V_{pp}$) and synchronously detecting the collected signal with a lock-in amplifier. When necessary, the spectra were numerically integrated.

The photoemission measurements were carried out at Berliner Elektronenspeicherring-Gesellschaft Für Synchrotronstrahlung m.b.H. (BESSY), where synchrotron radiation from the storage ring was dispersed by an SX700 monochromator and the photoelectrons detected by an hemispherical analyzer.

THE Fe/Si INTERFACE AT ROOM TEMPERATURE

Figure 1 shows a typical series of Auger spectra taken during Fe deposition on Si(100) at room temperature. The spectrum (a), corresponding to the clean Si surface, shows a sharp maximum at 87.3 eV, and other less pronounced structures at 41.5, 52.9, 70.5, 81.0, and 103.2 eV. All these peaks are due to Si L_{VV} Auger transitions,¹⁴ although those at 70.5 and 52.9 eV contain contributions from plasma losses of the main peak.¹⁵ Upon Fe deposition, a new maximum appears at 42.4 eV, corresponding to the M_{VV} Auger transition of Fe.¹⁶

The Fe coverage has been determined by using a previous Auger calibration.¹¹ In that work, we reported plots of the intensity of the main Fe and Si transitions (measured as the peak to peak height in the derivative spectra) as a function of the evaporation time where a clear break signalled the completion of the first Fe monolayer. However, after this point no more breaks could be distinguished, and the intensity evolution indicated that, above this coverage, the growth mode deviate from a layer-by-layer type.¹¹ The present data confirm those previous reports.

No LEED pattern can be seen after deposition of the first Fe monolayer, suggesting that the atoms in this layer do not sustain a large range order. Up to the coverages

measured in these experiments (~ 30 ML) no LEED pattern appears with further Fe deposition.

Auger transitions of the XVV type, involving the valence band, are very sensitive to changes in the valence-band density of states (DOS) projected locally on the atom where the initial core hole is produced.¹⁷ They are, therefore, suitable to detect the onset of reactions that modify the chemical environment of Si atoms. The kinetic energy of the main Si peak shifts continuously from 87.3 to 86.5 eV for Fe coverages up to 1.1 ML. In the range from 1.1 to 5.0 ML, the energy position remains constant at 86.5 eV. From 5.0 ML on, the energy diminishes again until, at ~ 7 ML, it saturates at 82.7 eV (see the inset in Fig. 1). The kinetic energy of an Auger transition can be written as $E_K(LVV) = E_L - 2E_V - V_{\text{eff}}$, where E_L is the energy of the core level, E_V the centroid of the valence-band DOS, and V_{eff} includes correlation effects (small for Si and Fe). During Fe-Si chemical bonding and silicide formation, both core level (E_L) and valence band (E_V) are modified (see below). Accordingly, we interpret the kinetic-energy shift as indicating the formation of some chemical compound between Si and Fe. The constant value between 1.1 and 5 ML indicates a stable chemical environment for the detected Si atoms, i.e., a compound of well-defined stoichiometry is formed at room temperature during Fe deposition from ~ 1 to ~ 5 ML.

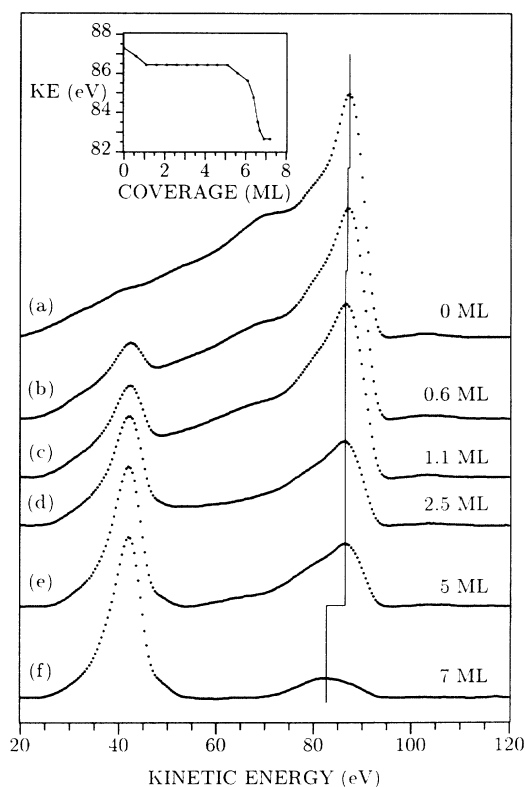


FIG. 1. Evolution of the low-energy Auger spectra in integral form (Fe $M_{23}VV$ and Si $L_{23}VV$) while depositing Fe on Si(100) at room temperature. The inset shows the shift in the kinetic energy of the main Si peak at a function of Fe coverage.

In Fig. 2 the evolution of the Si peak intensity is depicted logarithmically as a function of Fe coverage. The same three regions (0–1, 1–5, and from 5 ML on) can clearly be distinguished. The data confirm that the growth mode is not layer-by-layer (in this case only one linear region is expected¹¹). The experimental points for coverages between 0 and 1 ML can be fitted with a straight line; the attenuation coefficient obtained from its slope is $\alpha=0.60$. On the other hand, a linear fit to the points between 1 and 5 ML gives an attenuation coefficient $\alpha=0.78$. From 5 ML on, a value of $\alpha=0.55$, close to the initial one, results. From the measured values of the attenuation coefficients the average composition of the reacted layer can be obtained.

If we assume that the transmission of electrons of 87.3-eV kinetic energy through a complete and uniform Fe layer proceeds with a coefficient of 0.6, the larger value of α obtained between 1 and 5 ML would correspond to the transmission of electrons through a film whose relative Fe composition is 75%, the 25% left being Si atoms, i.e., the stoichiometry of this intermixed layer is Fe_3Si .

We can summarize the growth mode of Fe on Si(100) at room temperature as follows: the first Fe monolayer covers the Si surface almost uniformly, although in a disordered way, as evidenced by the absence of any LEED pattern. Further Fe evaporation produces a spontaneous reaction between Fe and Si at room temperature, to give an amorphous region (since no LEED pattern is seen) whose composition is close to Fe_3Si . Above a coverage of 5 ML the reaction slows down noticeably, and the Si dissolution in the overlayer diminishes, this latter being more and more Fe rich, until an almost uniform (although also disordered) and metallic Fe layer is formed. It is, however, remarkable that some Si signal is detected even after the deposition of 20 ML of Fe, indicating that still after this coverage there are some Si atoms dissolved in the Fe matrix.

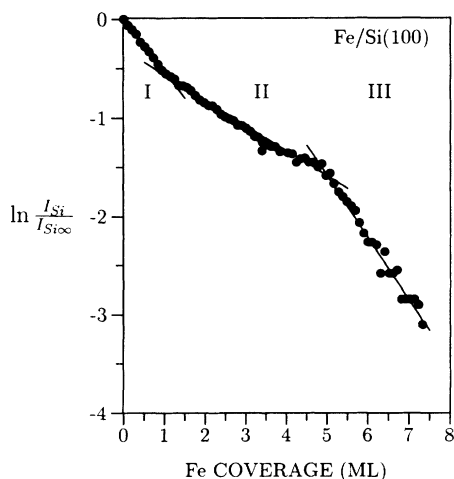


FIG. 2. Intensity (referred to the initial one) of the Si low-energy Auger transition while depositing Fe on Si(100). Regions I–III are discussed in the text. Region II reflects the formation at room temperature of a reacted silicidlike overlayer.

This mode of growth can explain the shifts in energy of the main Si peak shown in the right panel of Fig. 1. Between 0 and 1 ML, the energy position of the Si peak shifts in an almost continuous way to lower kinetic energy due to the growing number of Si atoms bonded to Fe. Between ~ 1 and ~ 5 ML, the energy position of the main peak remains constant, most of the signal being due to the Si atoms in the silicidlike layer. From this moment on, the detected signal is probably due to the Si atoms dissolved in the Fe matrix. The attenuation coefficient is again close to the original one, supporting this conclusion.

The proposed formation of a Fe_3Si compound can be confirmed by measuring the DOS at the valence band with photoemission. Figure 3 shows the evolution of the valence-band spectra, taken with a photon energy $h\nu=130$ eV, during the growth of Fe on Si(100). The spectrum (a) corresponds to the clean and 2×1 reconstructed Si(100) surface. The distance from the valence-band edge to the Fermi level, E_F-E_V , is 0.37 eV, in agreement with previous results.¹⁸ The peak at ~ 1 eV below E_F , labeled S_1 , is due to the emission from the dangling-bond surface states.¹⁸ Peak D , at ~ 7.5 eV, has been assigned to transitions from a high density of bulk states along $X-W$ without conservation of k_{\parallel} .¹⁹ The maximum B_1 (at ~ 2.8 eV) and the feature B_2 (at ~ 4.6 eV) are due to direct transitions from the bulk states.¹⁹

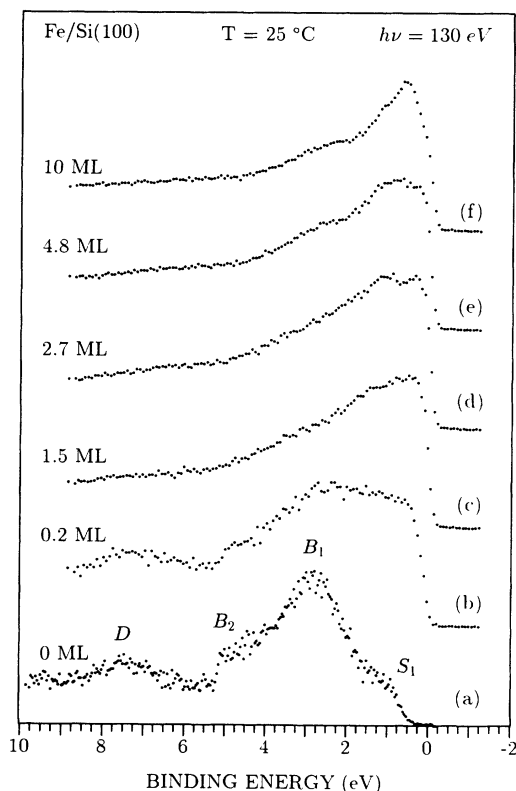


FIG. 3. Valence-band spectra taken during the deposition of Fe on Si(100) at room temperature. The photon energy was 130 eV, and the binding-energy scale is referred to the Fermi level. The spectra have been normalized to the same height.

After depositing 0.2 ML of Fe, the surface-state emission S_1 disappears and the valence-band edge moves closer to E_F , while a broad emission appears from 0.8 to 1.8 eV. For 1.5 ML of Fe, none of the features associated with bulk Si remain [the mean free path for electrons of 125-eV kinetic energy is ≈ 2 ML (Ref. 20)] while those of bulk Fe are not yet detected. There is a large peak at ~ 0.35 eV, with a weak structure at ~ 1.15 eV. At this coverage the surface can certainly be considered as metallic, due to a noticeable density of states at the Fermi level. At 2.7 ML, the spectrum is dominated by two peaks at 1.15 and 0.35 eV, respectively. After 4.8 ML, both peaks are less resolved due to the appearance of a new structure at 0.65 eV, assigned to Fe 3d states in bcc Fe, which dominates the spectrum at 10 ML. The line shape, width of the valence band, and peak positions of this latter spectrum, with a leading peak at 0.65 eV and a broader one at 2.6 eV are quite similar to those reported for clean Fe.^{21,22} In conclusion, the valence-band spectra taken after depositing 1.5, 2.7, and 4.8 ML of Fe show features that do not appear in the spectrum of clean Si nor in that of pure Fe. They reflect the formation of a silicelike layer, in accordance with the above-mentioned interpretation.

According to a detailed photoemission study of iron silicides,²³ the compound formed is not FeSi, nor β -FeSi₂. In Fe₃Si there are two inequivalent Fe atoms, one of them (with eight Fe atoms as nearest neighbors) displays a magnetic moment of $2.3\mu_B$, while the other (with four Si and four Fe atoms as nearest neighbors) has a smaller magnetic moment of $1.2\mu_B$.²⁴ Recent calculations for Fe₃Si (Ref. 25) have revealed that the DOS is clearly different for both Fe sites. In the vicinity of E_F this would lead to a two-peak structure with the same energy position (0.3–1.15 eV) than the one observed in the experimental valence-band spectrum. Accordingly, we identify the silicide formed at the interface during room-temperature deposition with Fe₃Si.

The evolution of the Si 2p core level with Fe deposition (Fig. 4) further confirms the formation of a reacted interface. At 1.5 ML of Fe the Si 2p core-level shifts ≈ 0.1 eV to lower binding energy. At 2.7 ML the shift of the main peak has increased to ≈ 0.25 eV, while the line shape clearly indicates the presence of a reacted component at lower binding energy. This component dominates the spectrum at 4.8 ML, and is shifted ≈ 0.5 eV to lower binding energy with respect to the bulk Si peak. The core-level shifts are due to charge transfer from Fe to Si during silicide formation. The onset of the reaction is detected at 1.5 ML, and, thus, it is found to coincide with the metallization of the overlayer as determined from the valence-band spectra. For 10-ML-thick films of Fe no signal from the Si 2p core level could be detected with $h\nu = 130$ eV.

The direct formation of a mixed amorphous interface has been predicted for metal/silicon interfaces produced by evaporation of the metal onto clean, cold Si substrates.²⁶ However, some results²⁷ indicate that a critical deposited thickness is necessary for the intermixing reaction to proceed. This critical thickness is the one required for the complete metallization of the overlayer. In

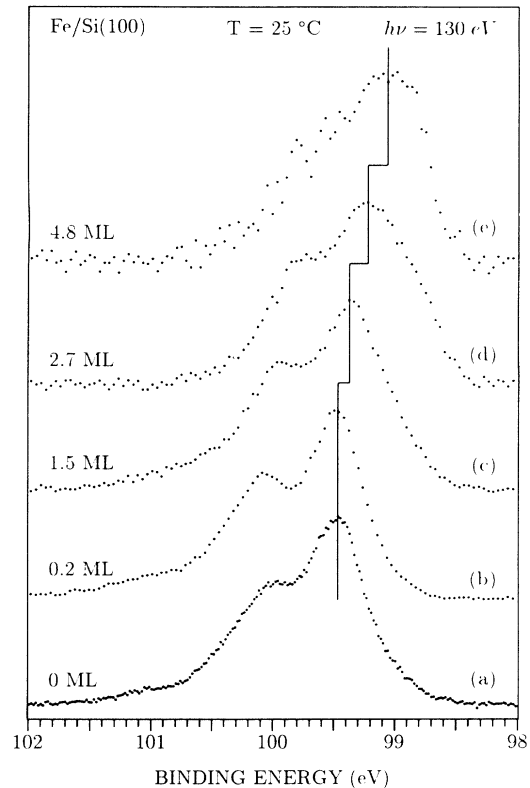


FIG. 4. Si 2p core-level spectra taken with $h\nu = 130$ eV during deposition of Fe on Si(100). The spectra have been normalized to the same height.

a metallic overlayer the delocalized conduction electrons screen the Si-Si bonds, producing their weakening and thus allowing the intermixing reaction to occur. The results of the work at hand are in accordance with this idea. In the Fe/Si case, the critical Fe coverage determined by AES seems to be ~ 1 ML of Fe, which coincides with the point where the surface can be taken as metallic, as evidenced by the photoemission data.

Similar results have recently been published for the Au/Si(111) interface.²⁸ In this case the critical Au thickness for chemical interaction is ≈ 2 Å, and is also explained in terms of the evolving electronic structure of Au with increasing Au coverage.

THE PHASE SEQUENCE OF IRON SILICIDES FORMATION

The fact that Fe₃Si forms right at the Fe/Si interface during room-temperature deposition of Fe may have profound influence in the sequence of formation of iron silicides during solid phase epitaxy (SPE). The sequence of formation is important to determine the amount of Si consumed in the reaction and the surface morphology of any given final product (i.e., β -FeSi₂).

The composition of the first silicide formed during annealing of a Fe/Si couple can be determined by AES. The evolution of the high-energy Fe LVV Auger spectra has been monitored during the annealing of a 30-ML Fe

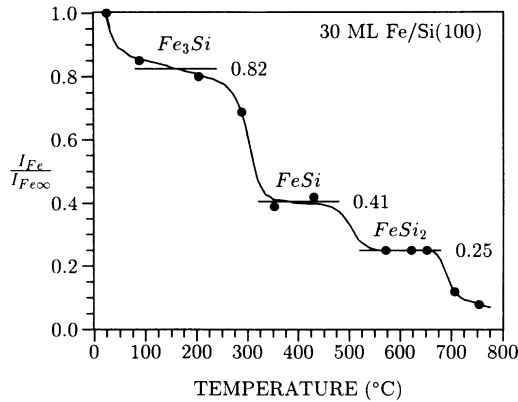


FIG. 5. Intensity evolution of the high-energy Fe Auger transition during annealing a 30-ML Fe film deposited on Si(100).

film deposited on Si(100). These spectra have been numerically integrated and the intensity of the highest energy peak (measured as the area between 660 and 740 eV) is depicted in Fig. 5 versus annealing temperature (the areas have been normalized to that of the Fe peak before annealing). There are plateaus on this plot where the intensity remains approximately constant. The first one ranges from 75 to 175°C, the second one from 350 to 450°C, and a last one from 550 to 650°C.

For a homogeneous film thicker than the corresponding electron mean free path, the intensities of the high-energy Auger peaks should be proportional to the number density of Fe in the film. This density is 8.46, 6.63, 4.42, and 2.66×10^{22} atoms/cm³ for Fe, Fe₃Si, FeSi, and FeSi₂, respectively, which are in a relation 1:0.78:0.52:0.31. The normalized intensities of the high-energy Fe peak measured in the different plateaus are 1, 0.82, 0.41, and 0.25, respectively. The agreement with the predicted values is excellent, assuring that the phases formed at 75–175°C, 350–450°C, and 550–650°C, are, respectively, Fe₃Si, FeSi, and FeSi₂. This result agrees with that of Ref. 9, the only difference being the formation of Fe₃Si at 100°C, which is absent in those results and, to our knowledge, in any other performed in UHV conditions. In this connection, we remark that for low

coverages (less than 10 ML) only the last two plateaus are seen.¹¹ This can be rationalized by realizing that, in these cases, the room-temperature interface composition is already close to Fe₃Si and, therefore, no abrupt changes in the Fe intensity are expected to occur at 100–200°C. For thicker films, although the composition of the layers near the Fe/Si interface is Fe₃Si, most of the deposited thickness is almost pure Fe, which then reacts with Si at 100–200°C to produce a thicker and more detectable Fe₃Si film.

Several phenomenological rules based in the equilibrium phase diagrams^{26,29} and in the heats of formation³⁰ have been formulated to explain the phase formation sequence in a metal/silicon interface. All of them predict FeSi as the first phase formed in the Fe/Si system. We have found conclusive experimental evidence that this is not the case, with Fe₃Si being actually the first formed phase. We propose that Fe₃Si is the first phase formed because: (i) it is already present at the room temperature Fe/Si interface, i.e., no nucleation barrier exists; and (ii) its crystallographic structure [Fe₃Si is cubic, with a lattice parameter of 5.656 Å, 16 atoms per unit cell, and a Fe-Fe nearest-neighbor distance of 2.83 Å (Ref. 31)] is very similar to that of pure Fe (bcc, a lattice parameter of 2.87 Å).

In summary, the Fe/Si(100) interface is reactive at room temperature. Upon deposition of Fe above 1 ML a spontaneous reaction occurs which results in formation of an amorphous silicide layer with a composition close to Fe₃Si. Above 5 ML the reaction slows down (at room temperature) and a film of metallic polycrystalline Fe film, with some Si dissolved, develops. During isochronal annealing of the Fe film, Fe₃Si forms first, followed by FeSi and FeSi₂, each on a well-defined (and coverage-dependent) temperature range.

ACKNOWLEDGMENTS

We are deeply indebted to Professor G. Kaindl, Dr. C. Laubschat, and Dr. S. Molodtsov for their invaluable help during measurements at BESSY. Financial support by the ESPRIT BRA 3026 and the CICYT is gratefully acknowledged.

¹M. C. Bost and J. E. Mahan, *J. Appl. Phys.* **58**, 2696 (1985).
²C. A. Dimitriadis, J. H. Werner, S. Logothetidis, M. Stutzmann, J. Weber, and R. Nesper, *J. Appl. Phys.* **68**, 1726 (1990).
³S. S. Lau, J. S. Y. Feng, J. O. Olowolafe, and M. A. Nicolet, *Thin Solid Films* **25**, 415 (1975).
⁴H. C. Cheng, T. R. Yew, and L. J. Chen, *J. Appl. Phys.* **57**, 12 (1985).
⁵C. A. Dimitriadis and J. H. Werner, *J. Appl. Phys.* **68**, 93 (1990).
⁶B. Li, M. Ji, J. Wu, and C. Hsu, *J. Appl. Phys.* **68**, 1099 (1990).
⁷M. de Crescenzi, G. Gaggiotti, N. Motta, F. Patella, A. Balzarotti, and J. Derrien, *Phys. Rev. B* **42**, 5871 (1990).
⁸Y. Ufuktepe and M. Onellion, *Solid State Commun.* **76**, 191 (1990).

⁹Q. G. Zhu, H. Iwasaki, E. D. Williams, and R. L. Park, *J. Appl. Phys.* **60**, 2629 (1986).
¹⁰A. Rizzi, H. Moritz, and H. Lüth, *J. Vac. Sci. Technol. A* **9**, 912 (1991).
¹¹J. M. Gallego and R. Miranda, *J. Appl. Phys.* **69**, 1377 (1991).
¹²T. Kanaji, T. Urano, A. Hiraki, and M. Iwami, in *Proceedings of the 8th International Vacuum Congress, 1980, Cannes, France*, edited by F. Abélès and M. Croset (Société Française du Vide, Paris, 1980), Vol. 1, p. 117.
¹³C. R. M. Grovenor, *Microelectronic Materials* (Hilger, Bristol, 1989).
¹⁴J. T. Grant and T. W. Haas, *Surf. Sci.* **23**, 347 (1970).
¹⁵B. A. Joyce and J. H. Neave, *Surf. Sci.* **27**, 499 (1971).
¹⁶G. W. Simmons and D. J. Dwyer, *Surf. Sci.* **48**, 373 (1975).
¹⁷M. C. Muñoz, V. Martínez, J. A. Tagle, and J. L. Sacedón, *J.*

- Phys. C **13**, 4247 (1980).
- ¹⁸F. J. Himpsel and D. E. Eastman, *J. Vac. Sci. Technol.* **16**, 1297 (1979).
- ¹⁹P. Koke, A. Goldmann, W. Mönch, G. Wolfgarten, and J. Pollmann, *Surf. Sci.* **152/153**, 1001 (1985).
- ²⁰M. P. Seah and W. A. Dench, *Surf. Interf. Anal.* **1**, 2 (1979).
- ²¹M. Pessa, P. Heimann and H. Neddermeyer, *Phys. Rev. B* **14**, 3488 (1976).
- ²²A. M. Turner and J. L. Erskine, *Phys. Rev. B* **30**, 6675 (1984).
- ²³J. Alvarez, J. J. Hinarejos, E. G. Michel, G. R. Castro, and R. Miranda, *Phys. Rev. B* **45**, 14 042 (1992).
- ²⁴W. A. Hines, A. H. Menotti, J. I. Budnick, T. J. Burch, T. Li-trenta, V. Niculescu, and K. Raj, *Phys. Rev. B* **13**, 4060 (1976).
- ²⁵J. Kudrnovsky, N. E. Christensen, and O. K. Andersen, *Phys. Rev. B* **43**, 5924 (1991).
- ²⁶R. M. Walser and R. W. Bené, *Appl. Phys. Lett.* **28**, 624 (1976).
- ²⁷A. Hiraki, *Surf. Sci. Rep.* **3**, 357 (1984).
- ²⁸S. L. Molodtsov, C. Laubschat, G. Kaindl, A. M. Shikin, and V. K. Adamchuk, *Phys. Rev. B* **44**, 8850 (1991).
- ²⁹M. Ronay, *Appl. Phys. Lett.* **42**, 577 (1983).
- ³⁰R. Pretorius, *Vacuum* **41**, 1038 (1990).
- ³¹B. Egert and G. Panzner, *Phys. Rev. B* **29**, 2091 (1984).